




A New Iterative Method for Free Vibration Analysis of a FG Timoshenko Beam

Hayrullah Gün Kadioğlu^a, M. Özgür Yaylı^b and Büşra Uzun^{c*}

^a Technical Sciences Vocational School, Department of Construction, İstanbul Arel University, İstanbul, Turkey

^{bc} Faculty of Engineering, Department of Civil Engineering, Bursa Uludag University, Bursa, Turkey

*✉: buzun@uludag.edu.tr  0000-0001-7370-2722, 0000-0003-2231-170X, 0000-0002-7636-7170 *

Received: 04.03.2025, Revised: 11.04.2025, Accepted: 11.04.2025

Abstract

In this study, the free vibration behavior of functionally graded Timoshenko beams is analyzed. The equations of motion are derived using Hamilton's principle, resulting in fourth-order differential equations. By solving these equations, displacement and rotation functions are obtained. Applying appropriate boundary conditions yields a system of four linear equations, which constitute the coefficient matrix for various support scenarios. The fundamental frequencies are determined by identifying the points where the determinant of this matrix equals zero. To efficiently locate these points, a novel iterative method is proposed. The results are validated through comparisons with existing studies in the literature and are illustrated with comprehensive tables and figures.

Keywords: Iterative method, functionally graded materials, Timoshenko beam theory, free vibration, frequency

1. Introduction

Composite materials have an important place in the design of structures and structural elements with advanced properties. Composite materials, which are used to meet the applications demanded in many fields, especially in engineering, have been frequently used in the modeling of various elements such as beams [1–7], shells [8–11], plates [12–16] etc. The mechanical properties of the components of classical composite materials change very sharply in the connection regions of the components. For this reason, problems such as stress concentrations and crack development may occur in these connection regions [17]. On the other hand, functionally graded (FG) composites, which were used for the first time in a spacecraft project in Japan in 1984, are special composites and prevent such problems [18]. Because the mechanical properties of the materials in the composition of functionally graded materials (FGMs) are constantly changing in a certain direction. This direction is usually the thickness direction for planar structural elements [19]. Due to superior properties, FGM is used in many fields such as biomedicine, optics, space, nuclear and automotive. It is a very interesting subject to explore the dynamic response of these materials used in all these areas [20–24]. Researchers have studied the free vibrations of FGMs using many different beam theories. The most well-known of these theories is the Euler-Bernoulli beam theory (EBBT). Many researchers refer to this theory as the classical beam theory. According to EBBT, a section that is perpendicular and plane to the neutral axis before bending is perpendicular and plane to the neutral axis after bending. It is said that bending occurs only with the effect of moment. On the other hand, in Timoshenko beam theory (TBT), which is the extended version of EBBT, a section that is perpendicular to the neutral axis and plane before bending remains plane after bending, but this



time it does not remain perpendicular to the neutral axis [25,26]. This shows that both shear force and moment influence bending. As is known, shear stresses are not constant. For this, a correction coefficient K_s is available to correct this stress distribution in the TBT [27]. In the light of all this information, it is seen that TBT is closer to reality and therefore always gives more accurate results than EBBT [28].

Various studies on a FG beam vibration can be referred when the literature is searched. Aydoğdu and Taşkın [29] have studied the vibration of a FGM beam with simply-supported at both ends using various higher-order beam theories. In the work, Hamilton's principle has utilized the equations of motion, and the beam frequencies have been found via the Navier-type solution method. Li [30] has proposed a solution method for the static and dynamic analyses of FGM beams in which shear deformations and rotational inertia effects are taken into account with Timoshenko's theory. A fourth-order differential equation has been derived as a mathematical model; displacement, rotation, internal forces, and stresses are defined as solutions to this equation. However, it only obtained results for simply-supported beams. Sina et al. [31] have proposed a new theory for the free vibration analysis of FGM beams, different from the traditional first-order beam theory. By assuming that the lateral normal stresses in the beam are zero, the equations of motion have been derived with the help of Hamilton's principles. Simsek [32] has analytically obtained the fundamental frequencies of FGM beams modeled with various higher-order theories of beam. Free vibration of FG beams considered with EBBT and TBT is investigated using Rayleigh–Ritz method by Pradhan and Chakraverty [33]. Thai and Vo [34] have used various high-order shear deformation theories available in the literature for bending and free vibration analyses of FGM beams. Nguyen et al. [35] have developed an analytical solution based on TBT for static and free vibration analysis of FGM beams under axial load. In the study, thanks to the transverse shear stiffness derived by utilizing the balance of shear strain energy, the correction factor in shear can be obtained analytically. Kahya and Turan [36] have developed a finite element solution for dynamic and stability of FG beams by using Timoshenko beam theory. Chen and Chang [37] have explored free vibration of beams by using the transformed section method and TBT. Hadji et al. [38] have studied a novel high-order shear deformation model for static and dynamic analyses of FG beams. Chen and Chang [39] have presented a closed form solution to find the natural frequencies of FG beams based on the EBBT. Lee and Lee [40] have investigated the free vibrations of FGM Euler-Bernoulli beams using the transfer matrix method. Celebi et al. [41] have proposed to use complementary functions method for vibration analysis of beams formed by FGMs. Wattanasakulpong and Ungbhakorn [42] have explored free vibration of Euler-Bernoulli beams under elastic boundary conditions via differential transformation method. Moreover, Wattanasakulpong and Prusty [43] have explored the free vibrations of layered FGM beams and experimentally confirmed their work. When looking at the literature review, various solution methods have been used to perform the analysis of FG beams. We can understand from other studies [44–59] in the literature that similar solution methods and mechanical analyses are frequently used in studies that take into account nano/micro structures as well as macro structures.

This study aims to contribute to the existing literature by developing a comprehensive vibration analysis framework for functionally graded Timoshenko and Euler-Bernoulli beams, in which material properties vary continuously according to a power-law distribution through the thickness. Unlike many previous works that rely on closed-form solutions or numerical approximations with limited boundary conditions, this research introduces an iterative solution technique that accommodates a variety of boundary conditions and provides results with high accuracy. The novelty of this study lies in the systematic formulation and frequency-dependent solution of the governing equations for different boundary scenarios, as well as in the comparative investigation of the influences of material gradation and geometric slenderness on the dynamic behavior of beams. The findings are expected to offer deeper insight into the

dynamic performance of FGM structures and to provide a practical analytical approach for engineering applications requiring high precision.

2. Functionally Graded Materials' Properties

The dimensions and coordinate axes for a typical rectangular FGM beam are shown in Fig. 1. It is considered that the FGM beam is linear elastic and the material properties change along the height as in Eq. (1) [37]:

$$P(z) = (P_c - P_m)V_c(z) + P_m \quad (1)$$

where, P_c and P_m show the material properties (modulus of elasticity E , Poisson's ratio μ , density ρ , shear modulus G) of ceramic and metal components, respectively. $V_c(z)$ indicates the volumetric material ratio of the ceramic in the composition and z denotes the thickness direction of the FG beam. $V_c(z)$, which varies depending on the direction of thickness, is expressed as follows [37]:

$$V_c(z) = \left(\frac{2z+h}{2h}\right)^k - \frac{h}{2} \leq z \leq \frac{h}{2} \quad (2a)$$

$$V_c + V_m = 1 \quad (2b)$$

In which, k is a non-negative number and it is called as power-law exponent. Additionally, h is the depth of the beam and V_m is the volumetric material ratio of the metal in the composition. Fig. 2 shows the variation of the ceramic component volumetric material ratio along the thickness of the FG beam with respect to k . While the change in variation of the volumetric material ratio is linear at $k=1$, a nonlinear change is seen at $k \neq 1$.

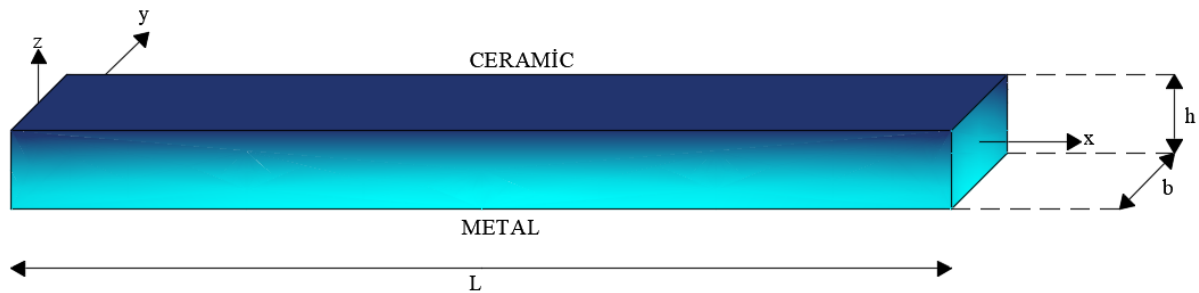


Fig. 1. A FG beam model

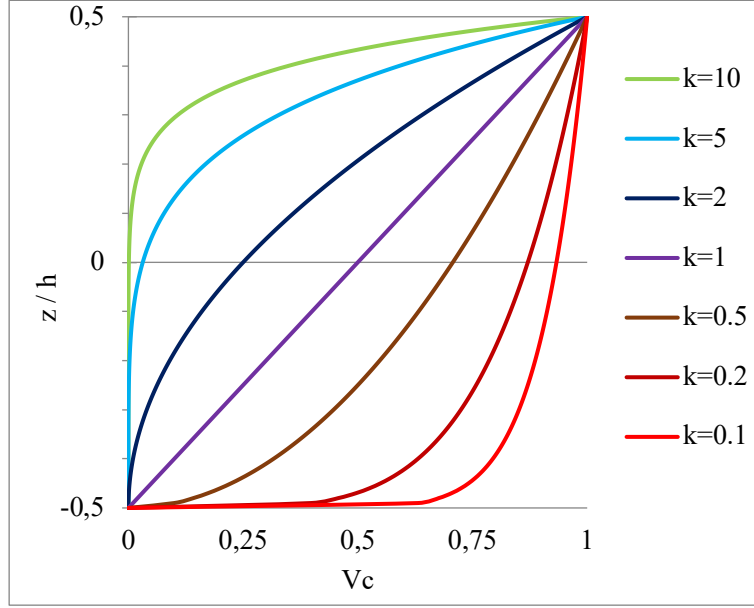


Fig. 2. Variation of the ceramic component volumetric material ratio versus z/h

Chen and Chang [37] have presented the following equations for FG Timoshenko beams with transformed section:

$$z_0 = \frac{k \left(1 - \frac{E_m}{E_C}\right) h}{2(k+2) \left(1 + k \frac{E_m}{E_C}\right)} \quad (3a)$$

$$A_C = hb \left(\frac{E_m}{E_C} + \left(1 - \frac{E_m}{E_C}\right) \left(\frac{1}{1+k}\right) \right) \quad (3b)$$

$$I_f = \frac{bh^3}{12} \left(\frac{E_m}{E_C} + 12 \left(1 - \frac{E_m}{E_C}\right) \left(\frac{1}{3+k} - \frac{1}{2+k} + \frac{1}{4(1+k)} \right) - \frac{3k^2 \left(1 - \frac{E_m}{E_C}\right)^2}{(1+k)(2+k)^2 \left(1 + k \frac{E_m}{E_C}\right)} \right) \quad (3c)$$

$$M_f = \rho A = hb\rho_C \left[\frac{\rho_m}{\rho_C} + \left(\frac{1}{1+k}\right) \left(1 - \frac{\rho_m}{\rho_C}\right) \right] \quad (3d)$$

$$J = \rho I = \frac{bh^3}{12} \rho_C \left(\begin{aligned} & \frac{\rho_m}{\rho_C} \left(4 - 12 \left(\frac{2z_0+h}{2h} \right) + 12 \left(\frac{2z_0+h}{2h} \right)^2 \right) \\ & + \left(1 - \frac{\rho_m}{\rho_C} \right) \left(\frac{12}{3+k} - \frac{24}{2+k} \left(\frac{2z_0+h}{2h} \right) + \frac{12}{1+k} \left(\frac{2z_0+h}{2h} \right)^2 \right) \end{aligned} \right) \quad (3e)$$

Where, z_0 is the area of the transformed section, A_C is the effective second moment of area about the neutral axis of this transformed area, I_f is the moment of inertia M_f is the corresponding mass per unit length of the FGM beam J is mass moment of inertia per unit length of the beam.

3. Background of Theory

In this part of the paper, the formulations of Timoshenko beam theory are presented for the free vibration problem. According to the TBT, displacements of the thick beam at any point not on its neutral axis are defined as follows [21]:

$$U(x, z, t) = u_0 + z\theta(x, t) \quad (4a)$$

$$W(x, z, t) = \varphi(x, t) \quad (4b)$$

here, $\varphi(x, t)$ is the transverse displacement and $\theta(x, t)$ is the rotation because of bending. u_0 indicates displacement because of in-plane elongating and t denotes time. It does not consider at here. If strains are obtained from displacements. Strains functions can be expressed as follows:

$$e_{xx} = z \frac{\partial \theta}{\partial x} \quad (5a)$$

$$e_{xz} = \frac{\partial \varphi}{\partial x} + \theta \quad (5b)$$

here e_{xx} and e_{xz} represent strain functions and they are re-written as follows:

$$e_{xx} = \partial U / \partial x \quad (6a)$$

$$e_{xz} = \partial W / \partial x + \partial U / \partial z \quad (6b)$$

The normal stress (σ_{xx}) and the transverse shear stress (σ_{xz}) are expressed as follows, respectively:

$$\sigma_{xx} = E e_{xx} \quad (7a)$$

$$\sigma_{xz} = K_S G e_{xz} \quad (7b)$$

where, K_S denotes the shear correction coefficient of Timoshenko. The shear correction factor varies depending on the geometry of the cross-section. Therefore, each geometric shape has its own specific shear correction factor. For instance, for a beam with a rectangular cross-section, the shear correction factor is typically taken as 5/6. By substituting Eqs. (6a) and (6b) into (7a) and (7b), the normal and transverse shear stresses are re-written as follows:

$$\sigma_{xx} = E z \frac{\partial \theta}{\partial x} \quad (8a)$$

$$\sigma_{xz} = K_S G \left(\frac{\partial \varphi}{\partial x} + \theta \right) \quad (8b)$$

If the moment and shear force are passed through the stresses.

$$M = \int_A z \sigma_{xx} dA = EI \frac{\partial \theta}{\partial x} \quad (9a)$$

$$V = \int_A \sigma_{xz} dA = K_S G A \left(\frac{\partial \varphi}{\partial x} + \theta \right) \quad (9b)$$

In Eq. (9a), I is the moment of inertia, A is the area of cross section, M is the bending moment and V is the shear force. The strain energy U is expressed as follows [21]:

$$U = \frac{1}{2} \int_0^L \int_A (\sigma_{xx} e_{xx} + \sigma_{xz} e_{xz}) dA dx = \frac{1}{2} \int_0^L M \frac{\partial \theta}{\partial x} + V \left(\frac{\partial \varphi}{\partial x} + \theta \right) dx \quad (10)$$

If simple harmonic motion is considered, the following relations are written:

$$\varphi(x, t) = \bar{\varphi}(x) e^{i\omega t} \quad (11a)$$

$$\theta(x, t) = \bar{\theta}(x) e^{i\omega t} \quad (11b)$$

in which, ω is the circular frequency, $\bar{\varphi}(x) = \bar{\varphi}$ and $\bar{\theta}(x) = \bar{\theta}$ are the displacement and rotation functions, respectively. By using these functions and the effect of rotary inertia is included, the kinetic energy equation (T) is expressed as follows:

$$T = \frac{1}{2} \int_0^L (\rho A \omega^2 \bar{\varphi}^2 + \rho I \omega^2 \bar{\theta}^2) dx \quad (12)$$

Where, ρ defines density of material. According to Hamiltonian's principle, $\delta = (T - U)$ eques zero.

$$\int_0^L \left(-M \frac{\delta d\bar{\theta}}{dx} - V \left(\frac{\delta d\bar{\varphi}}{dx} + \delta \bar{\theta} \right) + \rho A \omega^2 \delta \bar{\varphi}^2 + \rho I \omega^2 \delta \bar{\theta}^2 \right) dx = 0 \quad (13a)$$

$$\int_0^L \left[\left(\frac{dM}{dx} - V + \rho I \omega^2 \bar{\theta} \right) \delta \bar{\theta} + \left(\frac{dV}{dx} + \rho A \omega^2 \bar{\varphi} \right) \delta \bar{\varphi} \right] dx - [M \delta \bar{\theta}]_0^L - [V \delta \bar{\varphi}]_0^L = 0 \quad (13b)$$

Based on the above equations, the following relations can be written:

$$\frac{dM}{dx} = V - \rho I \omega^2 \quad (14a)$$

$$\frac{dV}{dx} = -\rho A \omega^2 \bar{\varphi} \quad (14b)$$

When the moment and shear force are used, the equations of motion are get as follows [37]:

$$EI \frac{d^2 \bar{\theta}}{dx^2} - K_S GA \left(\frac{d\bar{\varphi}}{dx} + \bar{\theta} \right) + \rho I \omega^2 \bar{\theta} = 0 \quad (15a)$$

$$K_S GA \left(\frac{d^2 \bar{\varphi}}{dx^2} + \frac{d\bar{\theta}}{dx} \right) + \rho A \omega^2 \bar{\varphi} = 0 \quad (15b)$$

The derivation of the free vibration equations of the Timoshenko beam is shown above. In this section, the alteration of material properties is not included in the formulas when deriving the equations. As can be understood, two equations govern the vibration of Timoshenko beams.

4. General Solutions for Functionally Graded Timoshenko Beams

When the FGM properties given in the second section of the study are included in Eqs. (15a) and (15b), the following governing equations are obtained:

$$E_C I_f \frac{d^2 \bar{\theta}}{dx^2} - K_S G_C A_C \left(\frac{d\bar{\varphi}}{dx} + \bar{\theta} \right) + J \omega^2 \bar{\theta} = 0 \quad (16a)$$

$$K_S G_C A_C \left(\frac{d^2 \bar{\varphi}}{dx^2} + \frac{d\bar{\theta}}{dx} \right) + M_f \omega^2 \bar{\varphi} = 0 \quad (16b)$$

The above expressions are capable of analyzing the vibration of FG beams. The following parameters are used to make some simplifications:

$$\Omega = \frac{K_S G_C A_C}{E_C I_f} \quad (17a)$$

$$\eta^4 = \frac{M_f \omega^2}{E_C I_f} \quad (17b)$$

$$\xi = \frac{J}{M_f} \quad (17c)$$

Based on the above simplifications, governing equations are re-written as follows:

$$\frac{d^2 \bar{\theta}}{dx^2} - \Omega \left(\frac{d\bar{\varphi}}{dx} + \bar{\theta} \right) + \eta^4 \xi \bar{\theta} = 0 \quad (18a)$$

$$\Omega \left(\frac{d^2 \bar{\varphi}}{dx^2} + \frac{d\bar{\theta}}{dx} \right) + \eta^4 \bar{\varphi} = 0 \quad (18b)$$

Fourth-order differential equations of $\bar{\varphi}$ can be obtained by Eqs. (18a) and (18b):

$$\frac{(\eta^8 \xi - \eta^4 \Omega) \bar{\varphi}(x) + \eta^4 (1 + \xi \Omega) \bar{\varphi}(x)'' + \Omega \bar{\varphi}(x)^{(4)}}{\Omega} = 0 \quad (19)$$

When the fourth-order differential equation is solved, the displacement function is obtained as follows:

$$\bar{\varphi}(x) = C_1 e^{x\beta} + C_2 e^{-x\beta} + C_3 \text{Cos}[x\gamma] + C_4 \text{Sin}[x\gamma] \quad (20)$$

β , γ and the first two derivatives of $\bar{\varphi}(x)$ are calculated as follows:

$$\beta = \frac{\sqrt{-\eta^4 \xi - \frac{\eta^4}{\Omega} + \frac{\sqrt{\eta^4 (\eta^4 - 2\eta^4 \xi \Omega + 4\Omega^2 + \eta^4 \xi^2 \Omega^2)}}{\Omega}}}{\sqrt{2}} \quad (21a)$$

$$\gamma = \frac{\sqrt{\eta^4 \xi + \frac{\eta^4}{\Omega} + \frac{\sqrt{\eta^4 (\eta^4 - 2\eta^4 \xi \Omega + 4\Omega^2 + \eta^4 \xi^2 \Omega^2)}}{\Omega}}}{\sqrt{2}} \quad (21b)$$

$$\bar{\varphi}(x)' = e^{x\beta} \beta C_1 - e^{-x\beta} \beta C_2 - \gamma \text{Sin}[x\gamma] C_3 + \gamma \text{Cos}[x\gamma] C_4 \quad (21c)$$

$$\bar{\varphi}(x)'' = e^{x\beta} \beta^2 C_1 + e^{-x\beta} \beta^2 C_2 - \gamma^2 \text{Cos}[x\gamma] C_3 - \gamma^2 \text{Sin}[x\gamma] C_4 \quad (21d)$$

Similarly, fourth-order differential equations of $\bar{\theta}$ can be obtained by:

$$\frac{(\eta^8 \xi - \eta^4 \Omega) \bar{\theta}(x) + \eta^4 (1 + \xi \Omega) \bar{\theta}(x)'' + \Omega \bar{\theta}(x)^{(4)}}{\Omega} = 0 \quad (22)$$

When the fourth-order differential equation is solved, the rotation function is obtained as follows:

$$\bar{\theta}(x) = d_1 e^{x\beta} + d_2 e^{-x\beta} + d_3 \text{Sin}[x\gamma] + d_4 \text{Cos}[x\gamma] \quad (23a)$$

$$\bar{\theta}(x)' = e^{x\beta} \beta d_1 - e^{-x\beta} \beta d_2 + \gamma \text{Cos}[x\gamma] d_3 - \gamma \text{Sin}[x\gamma] d_4 \quad (23b)$$

The constants C_f and d_f ($f=1,2,3,4$) are not independent of one another. Thus when Eq. (22) is written as follow and substituting the $\bar{\theta}$ and $\bar{\varphi}$ functions in Eq. (24), d_f constants are found in terms of C_f constants.

$$\frac{d\bar{\theta}}{dx} = -\frac{d^2\varphi}{dx^2} - \frac{\eta^4}{\Omega} \bar{\varphi} \quad (24)$$

$$d_1 = \Psi_\beta C_1 \quad (25a)$$

$$d_2 = -\Psi_\beta C_2 \quad (25b)$$

$$d_3 = \Psi_\gamma C_3 \quad (25c)$$

$$d_4 = -\Psi_\gamma C_4 \quad (25d)$$

Where, Ψ_β and Ψ_γ are defined as follows:

$$\Psi_\beta = -\frac{(\eta^4 + \beta^2 \Omega)}{\beta \Omega} \quad (26a)$$

$$\Psi_\gamma = \frac{(\gamma^2 \frac{\eta^4}{\Omega})}{\gamma} \quad (26b)$$

Rotation function and the first variation of its can be written in terms of C_f as follows:

$$\bar{\theta}(x) = \Psi_\beta C_1 e^{x\beta} - \Psi_\beta C_2 e^{-x\beta} + \Psi_\gamma C_3 \sin[x\gamma] - \Psi_\gamma C_4 \cos[x\gamma] \quad (27a)$$

$$\bar{\theta}(x)' = e^{x\beta} \beta C_1 \Psi_\beta + e^{-x\beta} \beta C_2 \Psi_\beta + \gamma \cos[x\gamma] C_3 \Psi_\gamma + \gamma \sin[x\gamma] C_4 \Psi_\gamma \quad (27b)$$

In addition, the natural frequency and dimensionless natural frequency (λ) are given as follows:

$$\omega = \sqrt{\frac{\eta^4 E C I_f}{M_f}} \quad (28a)$$

$$\lambda = \frac{\omega L^2}{h} \sqrt{\frac{\rho_m}{E_m}} \quad (29b)$$

Fig. 3 and Table 1 show the boundary conditions considered in this work. By using these boundary conditions, coefficients matrices are obtained. The points where the determinants of these coefficients matrices are zero give the natural frequencies. However, obtaining these natural frequencies is not as easy as one might think. To do this, the equations resulting from the determinant result are taken as a function with λ (the fundamental frequency) variable. In the Excel program, λ is given as zero as the initial value and increased by equal amounts in the range of $\Delta=0.001$, λ values are found where the function is equal to zero. The function crosses zero in the range of values it changes from positive to negative or from negative to positive. As seen in Fig. 4, the λ value of the function that is smaller in absolute value is accepted as the value that makes the function zero

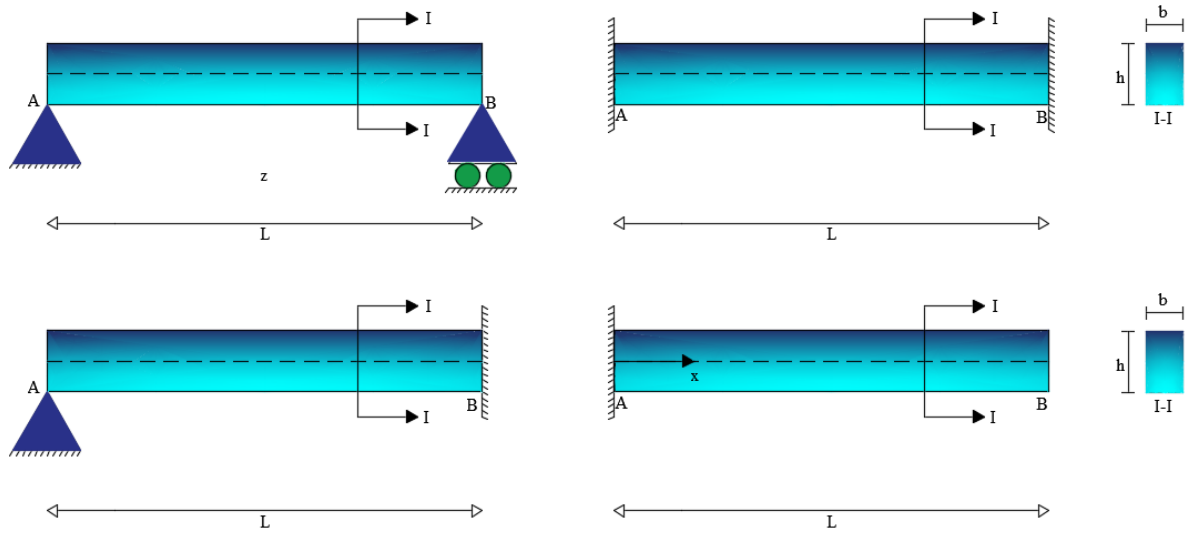


Fig. 3. Boundary conditions

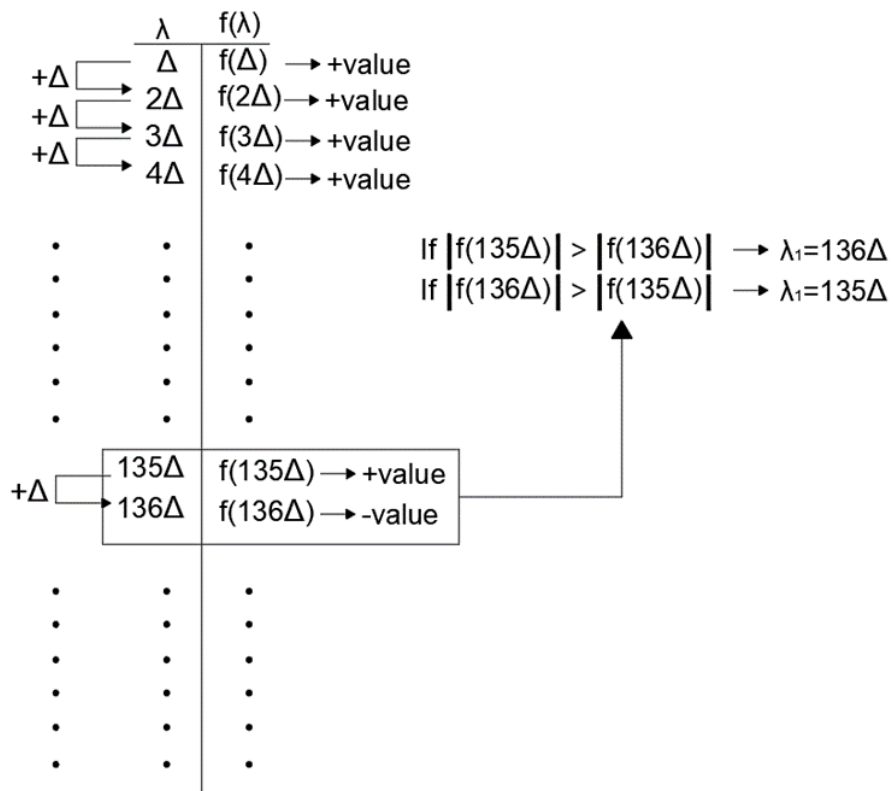


Fig. 4. An example of new exact iterative method

Table 1. Boundary conditions of the FG Timoshenko beams

Boundary Condition (B.C.)	x=0	x=L
Simply-Simply (S-S)	$\bar{\varphi} = 0 \ \& \ M = 0$	$\bar{\varphi} = 0 \ \& \ M = 0$
Clamped- Simply (C-S)	$\bar{\varphi} = 0 \ \& \ \bar{\theta} = 0$	$\bar{\varphi} = 0 \ \& \ M = 0$
Clamped-Clamped (C-C)	$\bar{\varphi} = 0 \ \& \ \bar{\theta} = 0$	$\bar{\varphi} = 0 \ \& \ \bar{\theta} = 0$
Clamped-Free (C-F)	$\bar{\varphi} = 0 \ \& \ \bar{\theta} = 0$	$M = 0 \ \& \ V = 0$

4.1. Simply-Supported Beams

The coefficients matrix is created by putting boundary conditions given in Table 1. Since the determinant of the coefficients matrix is equal to zero, Eq. (30b) is obtained.

$$\begin{pmatrix} 1 & 1 & 1 & 0 \\ e^{L\beta} & e^{-L\beta} & \text{Cos}[L\gamma] & \text{Sin}[L\gamma] \\ \beta\Psi_\beta & \beta\Psi_\beta & \gamma\Psi_\gamma & 0 \\ e^{L\beta}\beta\Psi_\beta & e^{-L\beta}\beta\Psi_\beta & \gamma\text{Cos}[L\gamma]\Psi_\gamma & \gamma\text{Sin}[L\gamma]\Psi_\gamma \end{pmatrix} \begin{pmatrix} C_1 \\ C_2 \\ C_3 \\ C_4 \end{pmatrix} = 0 \quad (30a)$$

$$-2\text{Sin}[L\gamma]\text{Sinh}[L\beta](\beta\Psi_\beta - \gamma\Psi_\gamma)^2 = 0 \quad (30b)$$

The exponential function in Eq. (30b) does not cross the horizontal axis. Since the points where Eq. (30b) is zero are searched, the equation can be simplified by excluding these exponential functions and functions that do not intersect the horizontal axis. Thus Eq. (31) is founded. Similar operations performed in this section are performed in other boundary conditions.

$$\text{Sin}[L\gamma] = 0 \quad (31)$$

In some dynamic studies based on beam theories, it has been observed that the equation governing the natural frequency of simply supported beams is the sine function [30,39].

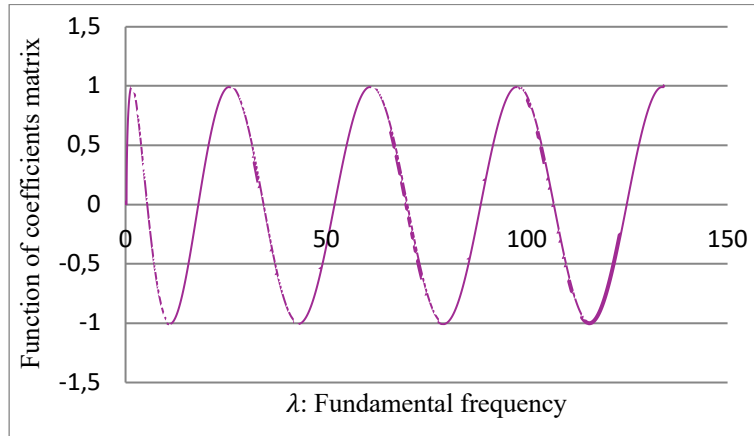


Fig. 5. Graph of the coefficients matrix function of a simply supported beam

Fig. 5 shows graphic of Eq. (31) dependent on the variable λ . To obtain Fig. 5 constants such as (E, G, K_S etc.) are substituted in the equation. Thus in Fig. 5, the points where the function intersects the λ -axis give the fundamental frequencies. To find these fundamental frequencies, the method mentioned in Chapter 4 has been used.

4.2. Clamped-Simply Supported Beams

The coefficients matrix of C-S beam is formed by putting related boundary conditions presented in Table 1. Since the determinant of the coefficients matrix is equal to zero, Eq. (32b) is obtained. Eq. (32c) is obtained when similar operations are applied for S-S beam.

$$\begin{pmatrix} 1 & 1 & 1 & 0 \\ e^{L\beta} & e^{-L\beta} & \cos[L\gamma] & \sin[L\gamma] \\ \Psi_\beta & -\Psi_\beta & 0 & -\Psi_\gamma \\ e^{L\beta}\beta\Psi_\beta & e^{-L\beta}\beta\Psi_\beta & \gamma\cos[L\gamma]\Psi_\gamma & \gamma\sin[L\gamma]\Psi_\gamma \end{pmatrix} \begin{pmatrix} C_1 \\ C_2 \\ C_3 \\ C_4 \end{pmatrix} = 0 \quad (32a)$$

$$e^{-L\beta}(\beta\Psi_\beta - \gamma\Psi_\gamma) \left((1 + e^{2L\beta})\sin[L\gamma]\Psi_\beta + (-1 + e^{2L\beta})\cos[L\gamma]\Psi_\gamma \right) = 0 \quad (32b)$$

$$\sin[L\gamma] + \frac{(-1+e^{2L\beta})}{(1+e^{2L\beta})} \cos[L\gamma] \frac{\Psi_\gamma}{\Psi_\beta} = 0 \quad (32c)$$

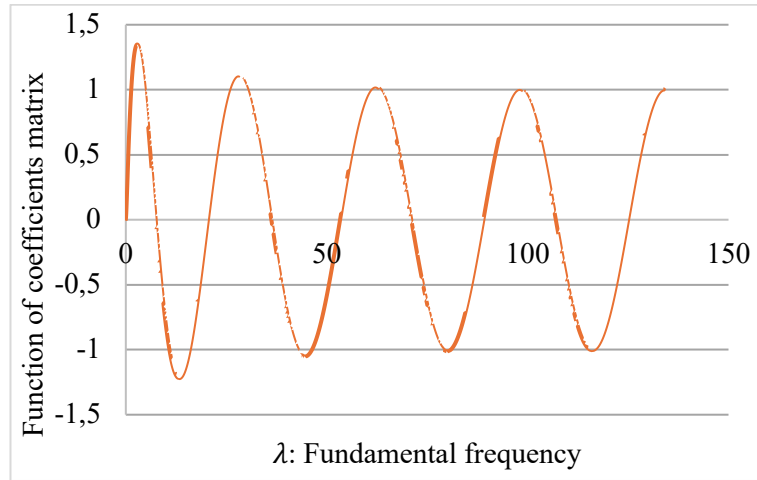


Fig. 6. Graph of the coefficients matrix function of a clamped- simply supported beam

Fig. 6 results when Eq. (32c) is drawn as a function dependent on the variable λ . Thus in the figure the points where the function intersects the λ -axis give the fundamental frequencies. To find these fundamental frequencies, the method mentioned in Chapter 4 has been used.

4.3. Clamped Beams

In this subsection, the coefficients matrix for C-C beam is shown. The coefficients matrix is created by putting boundary conditions for C-C beam given in Table 1. Since the determinant of the coefficients matrix is equal to zero, Eq. (33b) is obtained. Eq. (33c) is derived when similar steps are applied for S-S beam.

$$\begin{pmatrix} 1 & 1 & 1 & 0 \\ e^{L\beta} & e^{-L\beta} & \text{Cos}[L\gamma] & \text{Sin}[L\gamma] \\ \Psi_\beta & -\Psi_\beta & 0 & -\Psi_\gamma \\ e^{L\beta}\Psi_\beta & -e^{-L\beta}\Psi_\beta & \text{Sin}[L\gamma]\Psi_\gamma & -\text{Cos}[L\gamma]\Psi_\gamma \end{pmatrix} \begin{pmatrix} C_1 \\ C_2 \\ C_3 \\ C_4 \end{pmatrix} = 0 \quad (33a)$$

$$-4\Psi_\beta\Psi_\gamma + 4\text{Cos}[L\gamma]\text{Cosh}[L\beta]\Psi_\beta\Psi_\gamma + 2\text{Sin}[L\gamma]\text{Sinh}[L\beta](\Psi_\beta^2 - \Psi_\gamma^2) = 0 \quad (33b)$$

$$\frac{-4}{\text{Cosh}[L\beta]} + 4\text{Cos}[L\gamma] + \frac{2\text{Sin}[L\gamma](\Psi_\beta^2 - \Psi_\gamma^2)}{\text{Cosh}[L\beta]\Psi_\beta\Psi_\gamma} \text{Sinh}[L\beta] = 0 \quad (33c)$$

Fig. 7 results when Eq. (33c) is drawn as a function dependent on the variable λ . Thus in Fig. 7, the points where the function intersects the λ -axis give the fundamental frequencies.

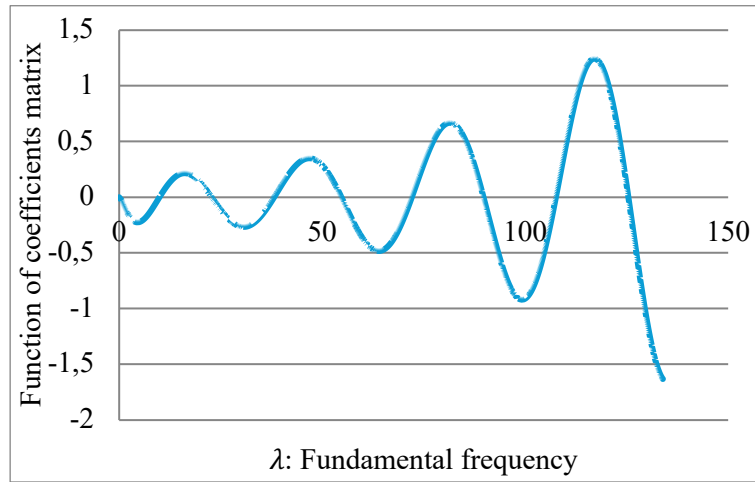


Fig. 7. Graph of the coefficients matrix function of a clamped supported beam

4.4. Clamped-Free Beams

The following equations belong to C-F beams. The coefficients matrix of C-F beam is created by putting boundary conditions written in Table 1. Since the determinant of the coefficients matrix is equal to zero, Eq. (34b) is obtained.

$$\begin{pmatrix} 1 & 1 & 1 & 0 \\ e^{L\beta}\beta\Psi_\beta & e^{-L\beta}\beta\Psi_\beta & \gamma\text{Cos}[L\gamma]\Psi_\gamma & \gamma\text{Sin}[L\gamma]\Psi_\gamma \\ \Psi_\beta & -\Psi_\beta & 0 & -\Psi_\gamma \\ e^{L\beta}\beta + e^{L\beta}\Psi_\beta & -e^{-L\beta}\beta - e^{-L\beta}\Psi_\beta & -\gamma\text{Sin}[L\gamma] + \text{Sin}[L\gamma]\Psi_\gamma & \gamma\text{Cos}[L\gamma] - \text{Cos}[L\gamma]\Psi_\gamma \end{pmatrix} \begin{pmatrix} C_1 \\ C_2 \\ C_3 \\ C_4 \end{pmatrix} = 0 \quad (34a)$$

$$e^{-L\beta} \left((-1 + e^{2L\beta})\text{Sin}[L\gamma]\Psi_\beta\Psi_\gamma(2\beta\gamma + \gamma\Psi_\beta - \beta\Psi_\gamma) - 2e^{L\beta}\Psi_\beta\Psi_\gamma(\beta^2 - \gamma^2 + \beta\Psi_\beta + \gamma\Psi_\gamma) - (1 + e^{2L\beta})\text{Cos}[L\gamma](\beta\gamma\Psi_\beta^2 - \beta\Psi_\beta^2\Psi_\gamma - \gamma(\beta + \Psi_\beta)\Psi_\gamma^2) \right) = 0 \quad (34b)$$

$$\frac{(-1+e^{2L\beta})\psi_\beta\psi_\gamma(2\beta\gamma+\gamma\psi_\beta-\beta\psi_\gamma)}{(1+e^{2L\beta})(\beta\gamma\psi_\beta^2-\beta\psi_\beta^2\psi_\gamma-\gamma(\beta+\psi_\beta)\psi_\gamma^2)} \text{Sin}[L\gamma] - \frac{2e^{L\beta}\psi_\beta\psi_\gamma(\beta^2-\gamma^2+\beta\psi_\beta+\gamma\psi_\gamma)}{(1+e^{2L\beta})(\beta\gamma\psi_\beta^2-\beta\psi_\beta^2\psi_\gamma-\gamma(\beta+\psi_\beta)\psi_\gamma^2)} - \text{Cos}[L\gamma] = 0 \quad (34c)$$

Fig. 8 results when Eq. (34c) is drawn as a function dependent on the variable λ . Thus in Fig. 8, the points where the function intersects the λ -axis give the fundamental frequencies.

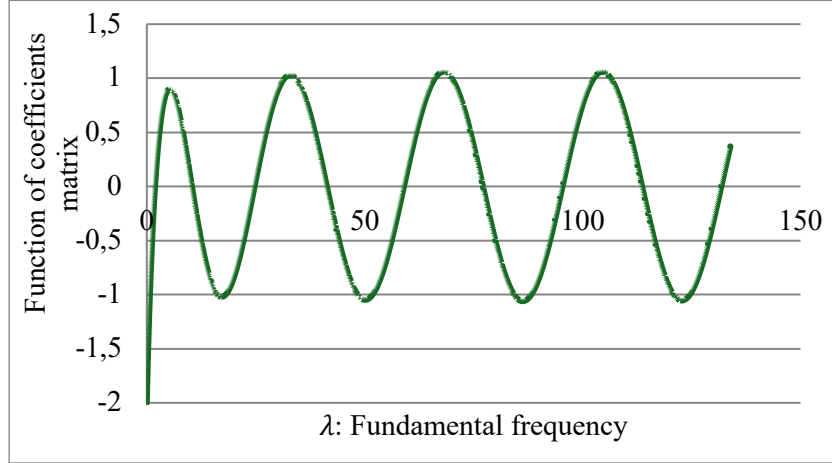


Fig. 8. Graph of the coefficients matrix function of a clamped- free supported beam

5. Results and Discussions

In this part, the results obtained from the study are presented in tables and graphs and compared with the studies in the literature. Firstly, the natural frequencies for the S-S beam are presented in Table 2 and compared with the studies in the literature. In order to reach the results in this table, the following material and geometrical properties are taken into account: $E_c=210$ GPa, $\rho_c=7850$ kg/m³, $E_m=70$ GPa, $\rho_m=2707$ kg/m³, $\mu_m=\mu_c=0.3$, $k=1$, $h=0.125$ m, $L=0.5$ m. As shown in Table 2, the results obtained in this study are in strong agreement with those reported in the existing literature. Owing to the iterative approach and the methodology employed, the results presented here are believed to offer higher accuracy and reliability compared to conventional analytical techniques.

Table 2. Comparison for natural frequencies of a S-S beam

Mode Number	ω (rad/s)		
	This study	Ref. [30]	Ref. [32]
1	6442.89	6457.93	6443.08
2	21471.27	21603.18	21470.95
3	39775.57	40145.42	39775.55
4	59092.41	59779.01	59092.37
5	78637.82	79686.16	78638.36

Secondly, Table 3 is shown to validate the accuracy of the method. Non-dimensional fundamental frequencies are obtained as follows in the study of Sina et al. [5] with the following parameters: $E_C = 380 \text{ GPa}$, $\rho_c = 3800 \text{ kg/m}^3$, $\mu_c = 0.23$, $E_m = 70 \text{ GPa}$, $\rho_m = 2700 \text{ kg/m}^3$, $\mu_m = 0.23$. Table 3 presents the results obtained in terms of the non-dimensional fundamental frequencies (ϖ) defined by:

$$\varpi = \omega L^2 \sqrt{\frac{I_1}{h^2 \int_{-h/2}^{h/2} E dz}} \quad I_1 = \int_{-h/2}^{h/2} \rho(z) dz \quad (35)$$

Table 3. Comparison of non-dimensional fundamental frequencies under various boundary conditions

	This study	Ref. [21]	Ref. [31]	Ref. [32]	Ref. [37]
S-S	2.702	2.745	2.702	2.695	2.803
S-C	4.134	4.203	4.140	-	4.291
C-C	5.848	5.954	5.869	5.811	6.078
C-F	0.971	0.986	0.970	0.969	1.008

Table 4. Variation of fundamental frequency according to k for S-S beams with $L/h=5$

Fundamental frequencies	Theory	Power-law exponent, k							
		0 (Ceramic)	0.2	0.5	1	2	5	10	∞ (Metal)
λ_1	TBT	5.152	4.805	4.408	3.990	3.635	3.431	3.314	2.677
[32] λ_1		5.153	4.807	4.408	3.990	3.634	3.4312	3.313	2.677
λ_2		17.871	16.741	15.428	14.007	12.718	11.312	11.312	9.286
λ_3		34.145	32.115	29.723	27.068	24.524	22.493	21.340	17.741
λ_4		51.813	48.883	45.405	41.467	37.525	34.065	32.096	26.922
λ_5	69.966	66.165	61.634	56.429	51.037	45.967	43.074	36.354	
λ_1	EBBT	5.395	5.020	4.593	4.149	3.780	3.595	3.492	2.803
[32] λ_1		5.395	5.022	4.594	4.148	3.779	3.595	3.492	2.803
λ_2		20.619	19.194	17.545	15.806	14.340	13.607	13.252	10.713
λ_3		43.348	40.371	36.864	33.100	29.865	28.248	27.604	22.524
λ_4		71.013	66.167	60.352	54.003	48.457	45.689	44.796	36.898
λ_5	101.545	94.657	86.250	76.936	68.695	64.594	63.516	52.762	

Finally, using the following material properties, fundamental frequencies are obtained in Tables 4-11 for S-S, C-S, C-C, C-F beams and compared with the different studies in the literature: $E_C = 380 \text{ GPa}$, $\rho_c = 3960 \text{ kg/m}^3$, $\mu_c = 0.30$, $E_m = 70 \text{ GPa}$, $\rho_m = 2702 \text{ kg/m}^3$, $\mu_m = 0.30$. By choosing a very large value of K_S , results have been obtained with in the EBBT. The results presented in these tables show clear consistency with those reported in previous studies in the literature. To better illustrate and interpret the key findings derived from the tabulated data, corresponding figures have been generated based on the tabular results.

Table 5. Variation of fundamental frequency according to k for S-S beams with L/h= 20

Fundamental frequencies	Theory	Power-law exponent, k							
		0 (Ceramic)	0.2	0.5	1	2	5	10	∞ (Metal)
λ_1	TBT	5.460	5.081	4.651	4.205	3.837	3.651	3.542	2.837
[32] λ_1		5.460	5.083	4.651	4.205	3.837	3.651	3.542	2.837
λ_2		21.573	20.086	18.393	16.634	15.172	14.411	13.965	11.209
λ_3		47.592	44.344	40.638	36.768	33.514	31.748	30.718	24.728
λ_4		82.440	76.887	70.527	63.846	58.153	54.903	53.018	42.835
λ_5		124.883	116.596	107.067	96.987	88.269	83.022	79.995	64.888
λ_1	EBBT	5.478	5.097	4.664	4.216	3.847	3.663	3.555	2.846
[32] λ_1		5.478	5.098	4.665	4.216	3.847	3.663	3.555	2.846
[42] λ_1		5.483	5.102	4.669	4.221	3.852	3.668	-	2.849
λ_2		21.844	20.325	18.599	16.810	15.334	14.596	14.168	11.350
[42] λ_2		21.933	20.408	18.676	16.884	15.407	14.670	-	11.396
λ_3		48.900	45.502	41.633	37.618	34.296	32.637	31.689	25.408
[42] λ_3		49.350	45.917	42.021	37.989	34.667	33.007	-	25.642
λ_4		86.325	80.331	73.491	66.376	60.473	57.524	55.878	44.854
[42] λ_4		87.734	81.631	74.703	67.536	61.629	58.680	-	45.586
λ_5		133.691	124.416	113.804	102.733	93.517	88.911	86.413	69.465
[42] λ_5	137.082	127.551	116.726	105.528	96.299	91.687	-	71.227	

Table 6. Variation of fundamental frequency according to k for C-S beams with L/h= 5

Fundamental frequencies	Theory	Power-law exponent, k							
		0 (Ceramic)	0.2	0.5	1	2	5	10	∞ (Metal)
λ_1	TBT	7.436	6.957	6.404	5.814	5.290	4.941	4.735	3.864
λ_2		20.438	19.202	17.761	16.178	14.681	13.502	12.821	10.617
λ_3		36.221	34.147	31.698	28.948	26.225	23.859	22.507	18.820
λ_4		53.327	50.389	46.902	42.926	38.850	35.071	32.917	27.708
λ_5		71.100	67.247	62.731	57.521	52.035	46.689	43.641	36.912
λ_1	EBBT	8.354	7.774	7.111	6.420	5.844	5.556	5.400	4.341
λ_2		25.702	23.928	21.867	19.684	17.835	16.910	16.483	13.354
λ_3		49.894	46.473	42.424	38.059	34.291	32.408	31.696	25.925
λ_4		78.442	73.098	66.656	59.595	53.405	50.318	49.372	40.758
λ_5		109.450	102.037	92.953	82.856	73.900	69.445	68.330	56.869

Table 7. Variation of fundamental frequency according to k for C-S beams with L/h= 20

Fundamental frequencies	Theory	Power-law exponent, k							
		0 (Ceramic)	0.2	0.5	1	2	5	10	∞ (Metal)
λ_1	TBT	8.478	7.892	7.226	6.534	5.961	5.667	5.494	4.405
λ_2		27.010	25.160	23.052	20.856	19.018	18.034	17.456	14.034
λ_3		55.026	51.304	47.050	42.593	38.814	36.686	35.440	28.591
λ_4		91.372	85.283	78.296	70.926	64.585	60.816	58.620	47.476
λ_5		134.813	125.971	115.785	104.964	95.504	89.573	86.134	70.048
λ_1	EBBT	8.552	7.957	7.282	6.583	6.006	5.718	5.549	4.444
[42] λ_1		8.566	7.970	7.294	6.594	6.017	5.729	-	4.451
λ_2		27.616	25.696	23.513	21.251	19.382	18.449	17.908	14.349
[42] λ_2		27.760	25.828	23.637	21.369	19.500	18.567	-	14.424
λ_3		57.299	53.318	48.783	44.074	40.176	38.229	37.122	29.772
[42] λ_3		57.918	53.889	49.316	44.584	40.685	38.738	-	30.094
λ_4		97.254	90.502	82.793	74.768	68.106	64.776	62.930	50.533
[42] λ_4		99.043	92.153	84.333	76.242	69.574	66.244	-	51.462
λ_5		147.026	136.829	125.153	112.962	102.803	97.726	94.994	76.394
[42] λ_5		151.137	140.632	128.692	116.343	106.174	101.085	-	78.536

Table 8. Variation of fundamental frequency according to k for C-C beams with L/h= 5

Fundamental frequencies	Theory	Power-law exponent, k							
		0 (Ceramic)	0.2	0.5	1	2	5	10	∞ (Metal)
λ_1	TBT	9.907	9.296	8.586	7.817	7.106	6.570	6.253	5.147
[32] λ_1		10.034	9.418	8.701	7.925	7.211	6.668	6.341	5.214
λ_2		22.797	21.482	19.937	18.215	16.523	15.053	14.199	11.845
λ_3		38.160	36.037	33.539	30.705	27.816	25.131	23.591	19.823
λ_4		54.751	51.809	48.314	44.302	40.102	36.020	33.693	28.450
λ_5	72.070	68.286	63.782	58.566	52.991	47.384	44.188	37.447	
λ_1	EBBT	11.991	11.160	10.206	9.208	8.373	7.955	7.737	6.230
[32] λ_1		12.183	11.340	10.372	9.364	8.528	8.110	7.880	6.330
λ_2		31.206	29.056	26.547	23.886	21.604	20.468	19.967	16.215
λ_3		56.709	52.827	48.211	43.213	38.880	36.716	35.940	29.466
λ_4		86.022	80.170	73.086	65.292	58.436	55.020	54.026	44.696
λ_5	117.430	109.487	99.217	88.826	79.141	74.327	73.179	61.016	

Table 9. Variation of fundamental frequency according to k for C-C beams with L/h= 20

Fundamental frequencies	Theory	Power-law exponent, k							
		0 (Ceramic)	0.2	0.5	1	2	5	10	∞ (Metal)
λ_1	TBT	12.208	11.368	10.412	9.419	8.592	8.157	7.901	6.343
[32] λ_1		12.224	11.385	10.426	9.431	8.604	8.170	7.913	6.351
λ_2		32.924	30.686	28.132	25.465	23.216	21.972	21.239	17.107
λ_3		62.786	58.580	53.764	48.700	44.369	41.836	40.348	32.623
λ_4		100.471	93.848	86.236	78.174	71.166	66.833	64.298	52.204
λ_5		144.771	135.389	124.560	113.005	102.795	96.137	92.262	75.222
λ_1	EBBT	12.401	11.539	10.559	9.545	8.708	8.290	8.046	6.346
[32] λ_1		12.414	11.554	10.571	9.555	8.719	8.301	8.056	6.450
[42] λ_1		12.430	11.566	10.584	9.569	8.732	8.314	-	6.459
λ_2		34.046	31.679	28.988	26.196	23.890	22.738	22.074	17.690
[42] λ_2		34.264	31.881	29.175	26.376	24.069	22.917	-	17.803
λ_3		66.341	61.732	56.481	51.023	46.503	44.245	42.969	34.471
[42] λ_3		67.172	62.499	57.195	51.707	47.185	44.927	-	34.902
λ_4		108.796	101.244	92.617	83.630	76.161	72.429	70.375	56.530
[42] λ_4		111.037	103.313	94.546	85.477	78.001	74.266	-	57.694
λ_5		160.942	149.782	136.995	123.632	112.486	106.915	103.942	83.625
[42] λ_5	165.915	154.337	141.262	127.640	116.503	110.935	-	86.210	

Table 10. Variation of fundamental frequency according to k for C-F beams with L/h= 5

Fundamental frequencies	Theory	Power-law exponent, k							
		0 (Ceramic)	0.2	0.5	1	2	5	10	∞ (Metal)
λ_1	TBT	1.898	1.768	1.620	1.465	1.336	1.267	1.226	0.986
[32] λ_1		1.895	1.766	1.617	1.463	1.334	1.265	1.224	0.985
λ_2		10.357	9.697	8.932	8.112	7.376	6.872	6.578	5.382
λ_3		24.736	23.251	21.507	19.585	17.763	16.330	15.511	12.855
λ_4		41.323	38.955	36.155	33.007	29.890	27.199	25.671	21.471
λ_5		59.008	55.750	51.880	47.463	42.943	38.785	36.425	30.660
λ_1	EBBT	1.942	1.807	1.654	1.494	1.363	1.297	1.259	1.009
[32] λ_1		1.939	1.804	1.651	1.491	1.360	1.294	1.257	1.007
λ_2		11.816	10.997	10.057	9.073	8.251	7.840	7.625	6.139
λ_3		31.218	29.067	26.556	23.886	21.612	20.475	19.974	16.220
λ_4		56.709	52.827	48.211	43.212	38.880	36.716	35.940	29.465
λ_5		86.022	80.170	73.086	65.292	58.436	55.020	54.026	44.696

Table 11. Variation of fundamental frequency according to k for C-F beams with L/h= 20

Fundamental frequencies	Theory	Power-law exponent, k							
		0 (Ceramic)	0.2	0.5	1	2	5	10	∞ (Metal)
λ_1		1.950	1.814	1.660	1.501	1.370	1.304	1.265	1.013
[32] λ_1		1.950	1.815	1.660	1.501	1.370	1.304	1.265	1.013
λ_2		12.088	11.253	10.304	9.319	8.501	8.079	7.830	6.281
λ_3	TBT	33.254	30.979	28.386	25.682	23.416	22.197	21.482	17.278
λ_4		63.581	59.286	54.375	49.224	44.850	42.375	40.930	33.036
λ_5		102.005	95.217	87.423	79.194	72.102	67.867	65.407	53.001
λ_1		1.953	1.817	1.663	1.503	1.372	1.306	1.267	1.015
[32] λ_1		1.953	1.817	1.663	1.503	1.371	1.306	1.267	1.015
[42] λ_1		1.953	1.816	1.663	1.504	1.372	1.307	-	1.015
λ_2		12.214	11.364	10.400	9.401	8.576	8.165	7.924	6.346
[42] λ_2		12.242	11.390	10.424	9.424	8.599	8.188	-	6.361
λ_3		34.060	31.692	28.999	26.207	23.899	22.747	22.082	17.697
[42] λ_3	EBBT	34.278	31.893	29.187	26.386	24.079	22.926	-	17.810
λ_4		66.340	61.732	56.480	51.023	46.502	44.244	42.968	34.470
[42] λ_4		67.171	62.498	57.194	51.707	47.185	44.926	-	34.901
λ_5		108.796	101.245	92.617	83.630	76.161	72.429	70.375	56.530
[42] λ_5		111.037	103.313	94.547	85.474	77.998	74.267	-	57.694

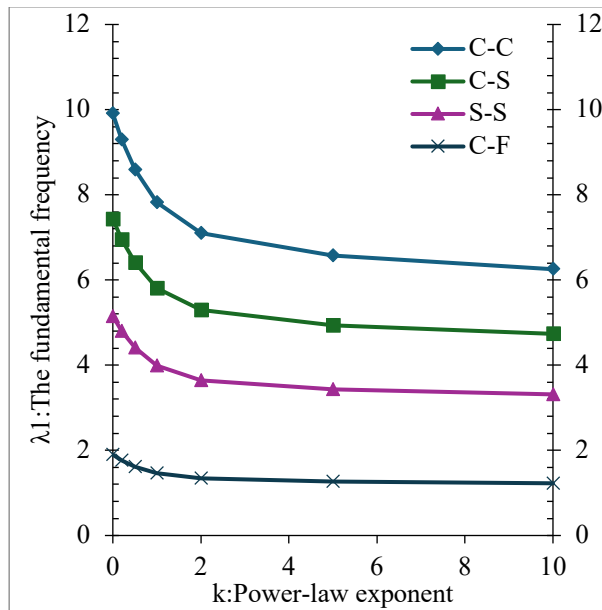


Fig. 9. Variation of the fundamental frequencies of FG Timoshenko beams in various support conditions in the first mode with respect to k.

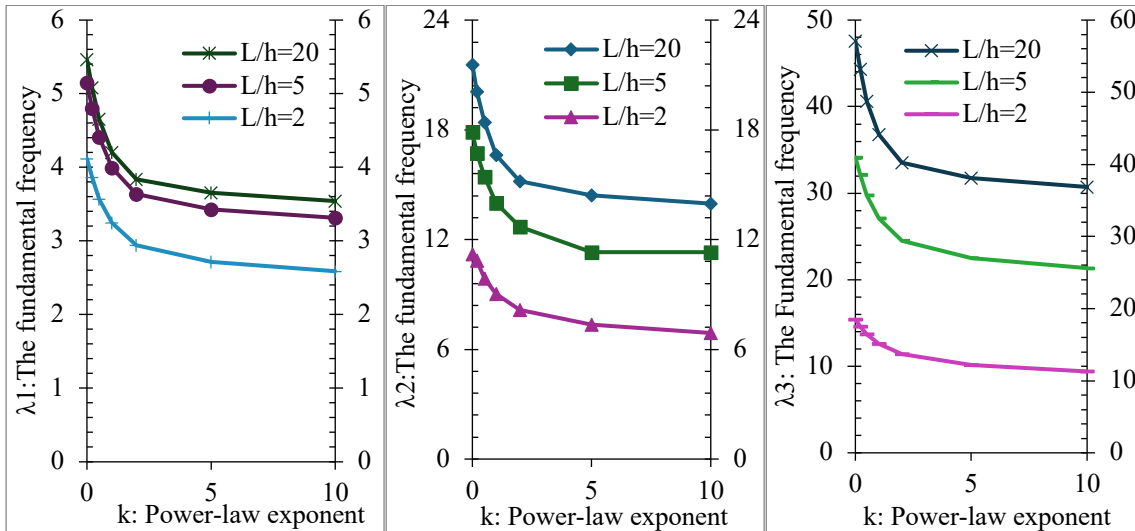


Fig. 10. Variation of the fundamental frequencies of S-S supported FG Timoshenko beams with different L/h in the first three modes with respect to k .

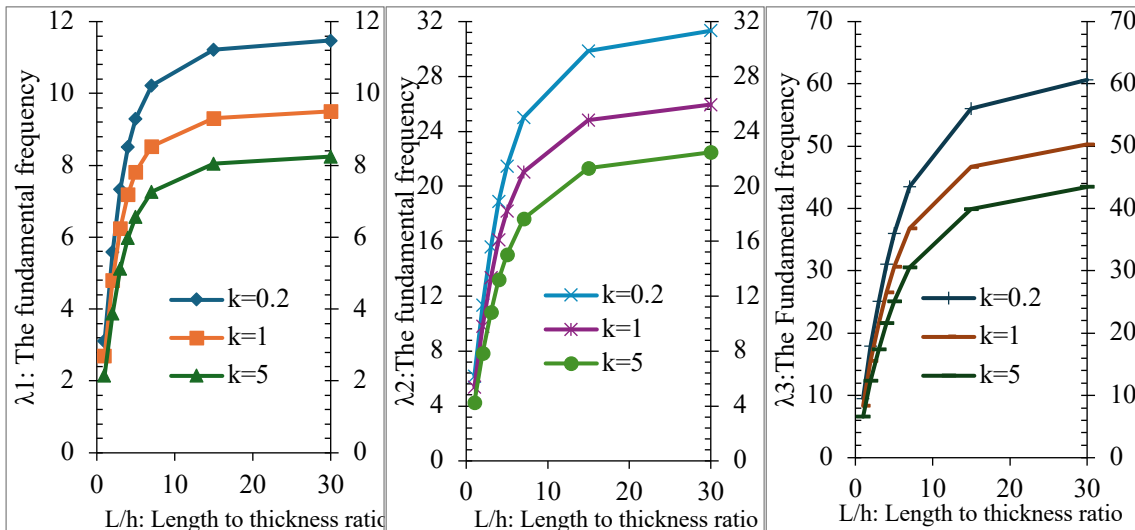


Fig. 11. Variation of the fundamental frequencies of C-C FG Timoshenko beams with different k in the first three modes with respect to L/h .

In Fig. 9 the variation of fundamental frequency for various support conditions is presented depending on k . It is observed that the largest fundamental frequency is in c-c supported beams, while the smallest fundamental frequency is found in C-F beams. As k decreases, the fundamental frequency decrease. In Fig. 10, the first three modes of k -dependent variation of S-S Timoshenko beams at different L/h values are given. In this figure, it is seen that the fundamental frequency increase as L/h increases. It has also been observed that the gap between the growth modes and fundamental frequency at different L/h values is widened. In Fig. 11 the fundamental frequency of the first three modes of C-C Timoshenko beams at various k values are shown depending on L/h . It is seen that the fundamental frequency increases as L/h increases. In Fig. 12 the fundamental frequency of S-S Euler-Bernoulli and Timoshenko beams are given depending on L/h . It is seen that the results of the two theories have converged as L/h increased. The researchers have seen that the results of EBBT and TBT at $L/h=20$ are very close to each other and $L/h=20$ is accepted as the critical value [16]. Fig. 13 indicates variation of fundamental frequency of clamped- simply and clamped-clamped supported FG Timoshenko and Euler-Bernoulli beams for $L/h=5$ in the first mode with respect to k . It cannot be said that

the variation of power-law exponent brings the fundamental frequency of Euler-Bernoulli and Timoshenko beams closer together or away from each other.

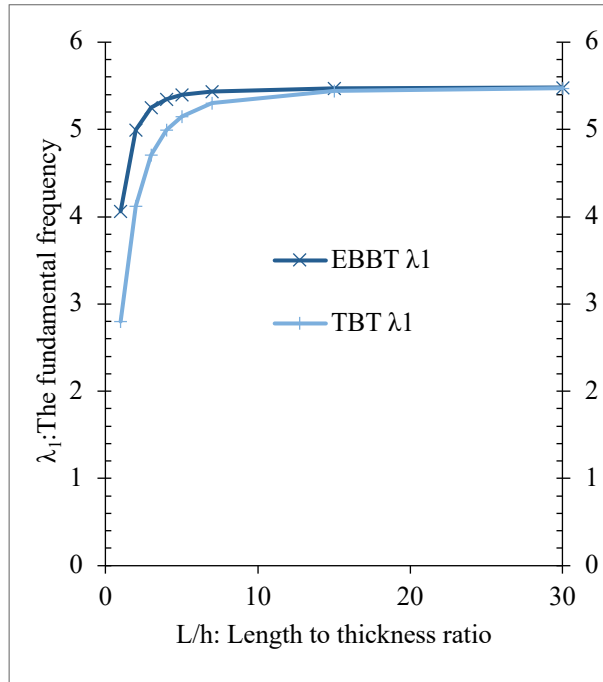


Fig. 12. Variation of the fundamental frequencies of S-S FG Timoshenko and Euler Bernoulli beams for $k=0$ in the first mode with respect to L/h .

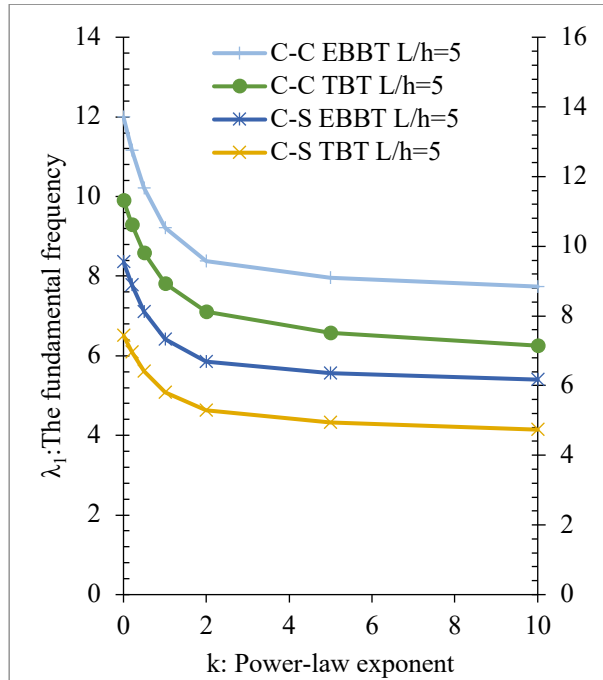


Fig. 13. Variation of the fundamental frequencies of C-S and C-C FG Timoshenko and Euler-Bernoulli beams for $L/h=5$ in the first mode with respect to k .

7. Conclusions

In this study, free vibration of FG Timoshenko and Euler-Bernoulli beams has been investigated. It is assumed that the material properties of the functionally graded beam change according to the force rule in the thickness direction according to the volume ratio of the components. Equations of motion have been obtained according to Timoshenko beam theory and these equations of motion have been solved by using the solution methods of differential equations. Thus, rotation and displacement functions are obtained. By incorporating boundary conditions into the problem formulation, frequency-dependent equations have been derived for each specific boundary condition. An iterative method has been proposed to solve these equations, yielding results that closely approximate the exact solutions. The accuracy of these results has been validated through comparison with findings from previous studies in the literature.

This method is believed to offer a promising approach for obtaining highly accurate results in analyses requiring precision.

In addition to these findings, other significant results obtained in this study are presented below in a structured format.

- As power-law exponent increases (material properties change from ceramic to metal), the fundamental frequencies decrease.
- The effect of the change of power-law exponent on the fundamental frequencies increases as the increase of mode.
- It cannot be said that the variation of power-law exponent brings the fundamental frequencies of Euler-Bernoulli and Timoshenko beams closer together or away from each other.
- If L/h increases, the fundamental frequencies increase.
- The fundamental frequencies found according to the Euler-Bernoulli beam theory are larger than those found according to the Timoshenko beam theory.
- As L/h increases, the fundamental frequencies of the Timoshenko beams and the fundamental frequencies of the Euler-Bernoulli beams converge. On the contrary, the results diverge as L/h decreases.
- The smallest the fundamental frequencies have been observed in the cantilever beam, and the largest the fundamental frequencies have been observed in the clamped beam.

Despite the promising outcomes, this study is subject to certain limitations. The analysis is confined to beams with material gradation following a power-law distribution through the thickness and assumes idealized boundary conditions. Effects such as temperature gradients, nonlinear material behavior, and three-dimensional stress states are not considered, which may influence the vibration characteristics in practical applications. Future research could address these aspects to enhance the applicability and robustness of the proposed method in more complex engineering scenarios.

Author Contribution

Hayrullah Gün Kadioğlu: Conducted a literature review, Designed and directed the paper, Verified the theories and methods, Conceived and designed the analysis, Performed the analysis, Wrote the paper, Prepared the paper for publication.

M. Özgür Yaylı: Conducted a literature review, Designed and directed the paper, Verified the theories and methods, Conceived and designed the analysis, Performed the analysis, Wrote the paper, Prepared the paper for publication.

Büşra Uzun: Conducted a literature review, Designed and directed the paper, Verified the theories and methods, Conceived and designed the analysis, Performed the analysis, Wrote the paper, Prepared the paper for publication.

References

- [1] Ermis M., Warping-included mixed FE approach of beating characteristics in functionally graded graphene platelet-reinforced composite spatially curved beams under harmonic excitation force. *94*(12), 3687-3713, Arch Appl Mech 2024.
- [2] Imran M., Khan R., Badshah S., Vibration Analysis of Cracked Composite Laminated Plate and Beam Structures. *Romanian Journal of Acoustics and Vibration*; *61*(3), 173-182, 2018.
- [3] Civalek Ö., Akbaş Ş. D., Akgöz B., Dastjerdi S., Forced Vibration Analysis of Composite Beams Reinforced by Carbon Nanotubes. *Nanomaterials* 2021;11:571.
- [4] Li M., Du S., Li F., Jing X., Vibration characteristics of novel multilayer sandwich beams: Modelling, analysis and experimental validations. *Mechanical Systems and Signal Processing*, 142, 106799, 2020.
- [5] Akbaş Ş. D., Dastjerdi, S., Akgöz, B., Civalek Ö., Dynamic Analysis of Functionally Graded Porous Microbeams under Moving Load. *Transp Porous Med*;142, 209–227, 2022.
- [6] Avcar M, Hadji L., Civalek Ö., Free vibration analysis of porous functionally graded sandwich beams. *Functionally Graded Structures: Modelling and computation of static and dynamical problems*, IOP Publishing, 2023.
- [7] İkinci B., Hadji L., İkinci B., Hadji L., Avcar M., Natural Frequency Analysis of Functionally Graded Porous Beams Using Hyperbolic Shear Deformation Theory, 2024.
- [8] Zhang C., Jin Q., Song Y., Wang J., Sun L., Liu H. and Guo, S., Vibration analysis of a sandwich cylindrical shell in hygrothermal environment. *Nanotechnology Reviews*, *10*(1), 414-430, 2021
- [9] Arefi M., Moghaddam S. K., Bidgoli E. M.-R., Kiani M., Civalek O., Analysis of graphene nanoplatelet reinforced cylindrical shell subjected to thermo-mechanical loads. *Composite Structures*, 255, 112924, 2021.

- [10] Sobhani E., Masoodi A. R., Civalek O., Ahmadi-Pari A. R., Agglomerated impact of CNT vs. GNP nanofillers on hybridization of polymer matrix for vibration of coupled hemispherical-conical-conical shells. *Aerospace Science and Technology*, 120, 107257, 2022.
- [11] Sayyad AS, Ghugal YM. Static and free vibration analysis of laminated composite and sandwich spherical shells using a generalized higher-order shell theory. *Composite Structures*, 219, 129-146, 2019.
- [12] Moradi-Dastjerdi R., Behdinan K., Temperature effect on free vibration response of a smart multifunctional sandwich plate. *Jnl of Sandwich Structures & Materials*, 23, 2399–421, 2021.
- [13] Mercan K., Baltacıoğlu A. K., Civalek Ö., Free vibration of laminated and FGM/CNT composites annular thick plates with shear deformation by discrete singular convolution method. *Composite Structures*,;186, 139–153, 2018.
- [14] Imran M, Khan R, Badshah S. Vibration Analysis of Cracked Composite Laminated Plate and Beam Structures. *Romanian Journal of Acoustics and Vibration* 2018;15:3–13.
- [15] Arefi M., Firouzeh S., Mohammad-Rezaei Bidgoli E., Civalek Ö., Analysis of porous micro-plates reinforced with FG-GNPs based on Reddy plate theory. *Composite Structures*, 247, 112391, 2020.
- [16] Civalek Ö., Dastjerdi ,S. and Akgöz B., Buckling and free vibrations of CNT-reinforced cross-ply laminated composite plates. *Mechanics Based Design of Structures and Machines* 50(6), 1914-1931, 2022.
- [17] Sankar B. V., An elasticity solution for functionally graded beams. *Composites Science and Technology*, 61(5), 689-696, 2001.
- [18] Yaylı M. Ö., Free vibration analysis of a rotationally restrained (FG) nanotube. *Microsystem Technologies*, 25, 3723-3734, 2019.
- [19] Loy, C. T., Lam, K. Y. and Reddy, J. N., Vibration of functionally graded cylindrical shells. *International Journal of Mechanical Sciences*, 41(3), 309-324, 1999.
- [20] Şimşek, M., Vibration analysis of a functionally graded beam under a moving mass by using different beam theories. *Composite structures*, 92(4), 904-917, 2010.
- [21] Su, H. and Banerjee, J. R., Development of dynamic stiffness method for free vibration of functionally graded Timoshenko beams. *Computers & Structures*, 147, 107-116, 2015.
- [22] Kitipornchai, S., Ke, L. L., Yang, J. and Xiang, Y., Nonlinear vibration of edge cracked functionally graded Timoshenko beams. *Journal of sound and vibration*, 324(3-5), 962-982, 2009.
- [23] Fang, J. S. and Zhou, D., Free vibration analysis of rotating axially functionally graded tapered Timoshenko beams. *International Journal of Structural Stability and Dynamics*, 16(05), 1550007, 2016.

- [24] Zahedinejad, P., Free vibration analysis of functionally graded beams resting on elastic foundation in thermal environment. *International Journal of Structural Stability and Dynamics*, 16(07), 1550029, 2016.
- [25] Wang, C. M., Zhang, Y. Y. and He, X. Q., Vibration of nonlocal Timoshenko beams. *Nanotechnology*, 18(10), 105401, 2007.
- [26] Wang, C. M., Reddy, J. N. and Lee, K. H., Shear Deformable Beams and Plates: Relationships with Classical Solutions. 23, 2001.
- [27] Timoshenko, S. P., LXVI. On the correction for shear of the differential equation for transverse vibrations of prismatic bars. *The London, Edinburgh, and Dublin Philosophical Magazine and Journal of Science*, 41(245), 744-746, 1921.
- [28] Kadioğlu, H. and Yaylı, M. Ö., Buckling analysis of non-local Timoshenko beams by using Fourier series. *International Journal of Engineering and Applied Sciences*, 9(4), 89-99, 2017.
- [29] Aydogdu, M. and Taskin, V., Free vibration analysis of functionally graded beams with simply supported edges. *Materials & design*, 28(5), 1651-1656, 2007.
- [30] Li, X. F., A unified approach for analyzing static and dynamic behaviors of functionally graded Timoshenko and Euler–Bernoulli beams. *Journal of Sound and vibration*, 318(4-5), 1210-1229, 2008.
- [31] Sina SA, Navazi HM, Haddadpour H. An analytical method for free vibration analysis of functionally graded beams. *Materials & Design* 2009;30:741–7. <https://doi.org/10.1016/j.matdes.2008.05.015>.
- [32] Şimşek, M., Fundamental frequency analysis of functionally graded beams by using different higher-order beam theories. *Nuclear Engineering and Design*, 240(4), 697-705, 2009.
- [33] Pradhan, K. K. and Chakraverty, S., Free vibration of Euler and Timoshenko functionally graded beams by Rayleigh–Ritz method. *Composites Part B: Engineering*, 51, 175-184, 2013.
- [34] Thai, H. T. and Vo, T. P., Bending and free vibration of functionally graded beams using various higher-order shear deformation beam theories. *International journal of mechanical sciences*, 62(1), 57-66, 2012.
- [35] Nguyen, T. K., Vo, T. P. and Thai, H. T., Static and free vibration of axially loaded functionally graded beams based on the first-order shear deformation theory. *Composites Part B: Engineering*, 55, 147-157, 2013.
- [36] Kahya, V. and Turan, M., Finite element model for vibration and buckling of functionally graded beams based on the first-order shear deformation theory. *Composites Part B: Engineering*, 109, 108-115, 2017.

- [37] Chen, W. R. and Chang, H., Vibration analysis of functionally graded Timoshenko beams. *International Journal of Structural Stability and Dynamics*, 18(01), 1850007, 2018.
- [38] Hadji, L., Khelifa, Z., & El Abbes, A. B., A new higher order shear deformation model for functionally graded beams. *KSCE Journal of Civil Engineering*, 20(5), 1835-1841, 2016.
- [39] Chen, W. R., and Chang, H., Closed-form solutions for free vibration frequencies of functionally graded Euler-Bernoulli beams. *Mechanics of Composite Materials*, 53, 79-98, 2017.
- [40] Lee, J. W. and Lee, J. Y., Free vibration analysis of functionally graded Bernoulli-Euler beams using an exact transfer matrix expression. *International Journal of Mechanical Sciences*, 122, 1-17, 2017.
- [41] Celebi, K., Yarimpabuc, D. and Tutuncu, N., Free vibration analysis of functionally graded beams using complementary functions method. *Archive of Applied Mechanics*, 88, 729-739, 2018.
- [42] Wattanasakulpong, N. and Ungbhakorn, V., Free vibration analysis of functionally graded beams with general elastically end constraints by DTM. *World Journal of Mechanics*, 2(6), 297-310, 2012.
- [43] Wattanasakulpong, N., Prusty, B. G., Kelly, D. W. and Hoffman, M., Free vibration analysis of layered functionally graded beams with experimental validation. *Materials & Design (1980-2015)*, 36, 182-190., 2012.
- [44] Akgöz, B. and Civalek, Ö., A microstructure-dependent sinusoidal plate model based on the strain gradient elasticity theory. *Acta mechanica*, 226, 2277-2294, 2015.
- [45] Yaylı, M. Ö., Aras, M. and Aksoy, S., An efficient analytical method for vibration analysis of a beam on elastic foundation with elastically restrained ends. *Shock and Vibration*, 2014(1), 159213, 2014.
- [46] Yaylı, M. Ö. and Çerçevik, A. E., Axial vibration analysis of cracked nanorods with arbitrary boundary conditions. *Journal of Vibroengineering*, 17(6), 2907-2921, 2015.
- [47] Yaylı, M., Buckling analysis of a rotationally restrained single walled carbon nanotube embedded in an elastic medium using nonlocal elasticity. *International Journal of Engineering and Applied Sciences*, 8(2), 40-50, 2016.
- [48] Yaylı, M. Ö., Buckling analysis of Euler columns embedded in an elastic medium with general elastic boundary conditions. *Mechanics Based Design of Structures and Machines*, 46(1), 110-122, 2018.
- [49] Söylemez, A. O. and Akgöz, B., Deflections of Cantilever Beams Subjected to A Point Load At the Free End. *International Journal of Engineering and Applied Sciences*, 16(3), 141-152, 2024.

- [50] Civalek, Ö., and Avcar, M., Free vibration and buckling analyses of CNT reinforced laminated non-rectangular plates by discrete singular convolution method. *Engineering with Computers*, 38(Suppl 1), 489-521, 2022
- [51] Yaylı M. Ö., Free Vibration Behavior of a Gradient Elastic Beam with Varying Cross Section. *Shock and Vibration*, 2014(1), 801696, 2014.
- [52] Yaylı, M. Ö. and Asa, E., Longitudinal vibration of carbon nanotubes with elastically restrained ends using doublet mechanics. *Microsystem Technologies*, 26, 499-508, 2020.
- [53] Yaylı, M. Ö., Yanik, F. and Kandemir, S. Y., Longitudinal vibration of nanorods embedded in an elastic medium with elastic restraints at both ends. *Micro & Nano Letters*, 10(11), 641-644, 2015.
- [54] Dastjerdi, S., Malikan, M., Akgöz, B., Civalek, Ö., Wiczenbach, T., and Eremeyev, V. A., On the deformation and frequency analyses of SARS-CoV-2 at nanoscale. *International Journal of Engineering Science*, 170, 103604, 2022.
- [55] Dastjerdi, S., Akgöz, B. and Civalek, Ö., On the shell model for human eye in Glaucoma disease. *International Journal of Engineering Science*, 158, 103414, 2021.
- [56] Alibakhshi, A., Dastjerdi, S., Akgöz, B. and Civalek, Ö., Parametric vibration of a dielectric elastomer microbeam resonator based on a hyperelastic cosserat continuum model. *Composite Structures*, 287, 115386, 2022.
- [57] Yaylı, M. Ö., Torsion of nonlocal bars with equilateral triangle cross sections. *Journal of Computational and Theoretical Nanoscience*, 10(2), 376-379, 2013.
- [58] Yaylı, M. Ö., Kandemir, S. Y. and Çerçevik, A. E., Torsional vibration of cracked carbon nanotubes with torsional restraints using Eringen's nonlocal differential model. *Journal of Low Frequency Noise, Vibration and Active Control*, 38(1), 70-87, 2019.
- [59] Yaylı, M. Ö., Kandemir, S. Y. and Çerçevik, A. E., Torsional vibration of cracked carbon nanotubes with torsional restraints using Eringen's nonlocal differential model. *Journal of Low Frequency Noise, Vibration and Active Control*, 38(1), 70-87, 2019.